

DOI: 10.1002/adfm.200600707

Molecular Barbed Wire: Threading and Interlocking for the Mechanical Reinforcement of Polymers**

By Nicholas T. Tsui, Lokman Torun, Brian D. Pate, Alex J. Paraskos, Timothy M. Swager,* and Edwin L. Thomas*

The incorporation of pendant iptycene units into polyesters creates a novel polymer-chain contour resembling “molecular barbed wire.” These types of units contain a unique structural property called the internal molecular-free volume (IMFV) and have been shown to induce steric interactions between polymer chains through the minimization of the IMFV. This process creates a sterically interconnected polymer-chain network with high ductility because of two new mechanisms: molecular threading and molecular interlocking. The ability for these mechanisms to enhance the mechanical properties of polyesters is robust across concentration and processing conditions. The size, shape, and concentration of these pendant units affect the mechanical behavior, and results indicate that the larger units do not necessarily produce superior tensile properties. However, the molecular-barbed-wire architecture consistently produces enhanced mechanical properties compared to the reference polyester. The particular stress–strain response can be tailored by minute changes to the periphery of the iptycene unit.

1. Introduction

Polymers are used in a wide range of applications, and enhancements to the mechanical properties improve both the performance and longevity of commercial products. Typically, with homopolymers, improvements to stiffness and ductility are mutually exclusive. The most common techniques to raise stiffness are increasing chain alignment,^[1,2] increasing crystallinity,^[3–5] or increasing the glass-transition temperature (T_g) to well above operating temperatures.^[6,7] Each of these approaches almost always results in a sacrifice in ductility. Strategies for enhancing ductility include the reverse of the techniques for increasing stiffness,^[8] introducing new deformation^[9] or length-scale-dependent deformation mechanisms,^[10] or increasing interchain interactions (e.g., lightly crosslinking or increasing the number of entanglements above the entanglement density).^[11–13] It is very rare and usually system specific when improvements to the mechanical properties of a homopolymer avoid the stiffness/ductility tradeoff.

Pendant units have been examined for their effects on the mechanical properties of polymers because the enhanced solubility rendered to the chain backbone facilitates processing of films and fibers. Studies show that the mechanical properties still follow the stiffness/ductility tradeoff^[14–17] and even sometimes sacrifice both.^[18] One particular structure that has been gaining interest is triptycene (T),^[19–25] which is characterized by its rigid, shape-persistent geometry. It differs from typical pendant groups because it contains a structural characteristic called the internal molecular-free volume (IMFV), defined as “the difference in volume between that which is generated by the geometry of a structure and that which is occupied by the structure itself” (Fig. 1).

We recently reported that T incorporated at 21 wt % into a polyester with a long aliphatic component resulted in excep-

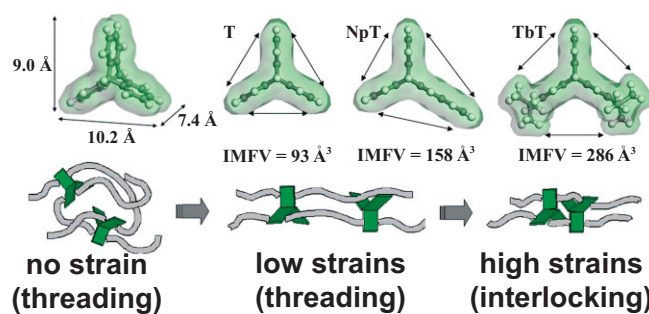


Figure 1. Iptycene units (T: triptycene, NpT: naphthalene-modified triptycene, and Tbt: *tert*-butyl-modified triptycene) with dimensions shown in 3D along with schematics of IMFV spaces marked off with arrows. Inherent IMFV values were calculated by using a method introduced in previous work [26] that only considers the isolated structural unit. Also shown is a schematic of triptycene incorporated into a polymer demonstrating new steric interactions between chains: molecular threading and molecular interlocking.

[*] Prof. T. M. Swager, Dr. L. Torun, Dr. A. J. Paraskos
Department of Chemistry
Massachusetts Institute of Technology
77 Massachusetts Ave., Cambridge, MA 02139 (USA)
E-mail: tswager@mit.edu

Prof. E. L. Thomas, N. T. Tsui, Dr. B. D. Pate
Department of Materials Science and Engineering
Massachusetts Institute of Technology
500 Technology Square, Cambridge, MA 02139 (USA)
E-mail: elt@mit.edu

[**] This work was supported by the U.S. Army Research Office through the Institute for Soldier Nanotechnologies under Contract DAAD-19-02-0002. We thank Dr. Wayne E. Marsh, Dr. Gregory T. Dee, Richard B. Maynard, and Charles W. Favorite from DuPont. We also acknowledge invaluable contributions from Dr. Alex J. Hsieh.

tionally enhanced values for Young's modulus (about 3 times), strength (about 3 times) and strain to failure (over 20 times) compared to the same polyester without T.^[26] This behavior was a consequence of the unique geometry of the T unit. The system's "desire" to minimize the overall IMFV resulted in the occupation of the T cavities with neighboring polymer chains, promoting new types of nanoscale steric interactions in the polyester studied. The specific interactions induced by the presence of IMFV were molecular threading and molecular interlocking (shown schematically in Fig. 1). Both types of interactions are means to enhance lateral interactions between polymer chains without covalent chemical bonds. Molecular threading is a result of T-chain interactions, and molecular interlocking results from T-T interactions. The presence of shape-persistent pendant units with IMFV (like T) spaced relatively far apart from one another produces a polymer chain that resembles "molecular barbed wire", in contrast to the typical "smooth" polymer-chain contour (Fig. 2).



Figure 2. Schematic of pendant units with IMFV generating a polymer-chain contour resembling "molecular barbed wire".

In this paper, we demonstrate that molecular barbed wire can be constructed from a number of different types of pendant units. We investigate how varying the amount of IMFV in the pendant unit affects the molecular-threading and molecular-interlocking phenomena. We also examine how the mechanical properties progress amongst these polymers, all of which exhibit superior mechanical properties compared to a polymer without such modifications. We show that by simply adjusting the IMFV of the pendant unit, the stress response at any given strain can be tailored to meet a particular application requirement.

2. Results and Discussion

Three types of polyesters with various iptycene units were prepared and characterized against an analogous reference polyester backbone with a benzene unit instead of an iptycene (Fig. 3).

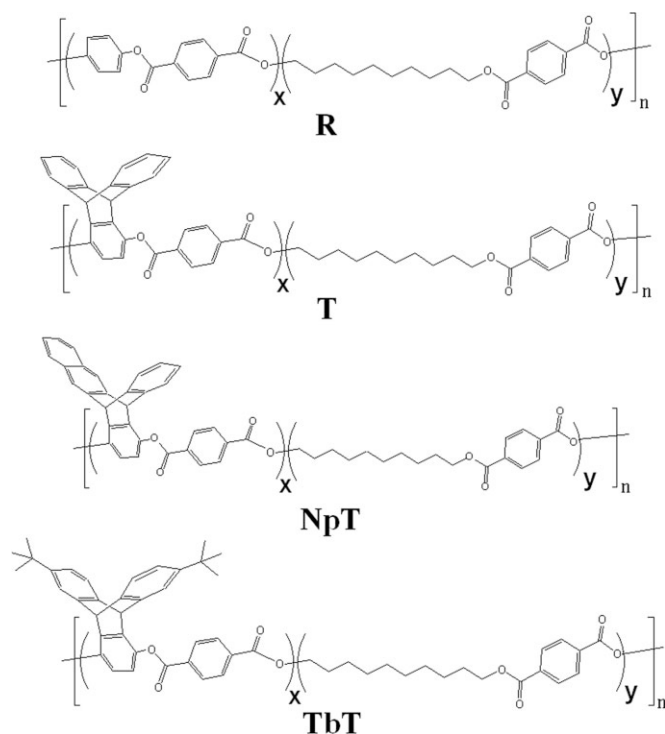


Figure 3. Chemical structures of the reference (R) non-triptycene (NT) polyester, T, NpT, and TbT. x and y can be varied to obtain different iptycene concentrations. " x/y " polyester film notations refer to this ratio.

The first two polyesters (reference non-T (NT) and T) were similar to those studied previously but with a greater ratio of the aliphatic component (Fig. 3: $x/y=1/5$ here versus $1/3$ in Tsui et al.)^[26] Two new types of iptycene units were synthesized (naphthalene-modified T (NpT) and *tert*-butyl-modified T (TbT)) to create a range in size and shape of the pendant units, resulting overall in three different types of molecular barbed wire. The aromatic components (which include the pendant units) are distributed through approximate statistically random copolymerization; therefore, the chemical structures represented in Figure 3 reflect this approximation. The molecular weights of the four polymers are listed in Table 1.

Samples were initially prepared by solvent-casting from dichloromethane, as in previous work with T and reference NT polyesters.^[26] But unlike the previous study, all three iptycene-containing polyester films were opaque and brittle. This sol-

Table 1. Molecular weights of polyesters.

| Sample | M_n [g mol ⁻¹] | M_w [g mol ⁻¹] | PDI |
|-----------|------------------------------|------------------------------|------|
| 1/3 R [a] | 31,900 | 62,000 | 1.94 |
| 1/3 T [a] | 40,300 | 75,500 | 1.87 |
| 1/5 R | 32,000 | 61,900 | 1.93 |
| 1/5 T | 31,200 | 56,700 | 1.82 |
| 1/5 NpT | 29,500 | 62,200 | 2.11 |
| 1/5 TbT | 26,800 | 49,600 | 1.85 |

[a] Data from previous study on solvent-cast films.^[26]

vent-induced crystallinity is likely to have been caused by the lower molecular weights and lower iptycene content of the polyesters in this work. Therefore, the solvent-cast films were melted at 150 °C and then quickly cooled to room temperature in order to depress the crystalline component evidenced in differential scanning calorimetry (DSC; Table 2). This treatment produced robust films more suitable for reliable mechanical testing.

The melt-pressed film of the reference polyester was cloudy-white because of its crystallinity. The iptycene films were all clear but had a slight yellowish tint. Thermogravimetric analysis (TGA; Table 2) indicated that these polymers are stable in air at temperatures well above the processing conditions, so this yellow tint is caused by residual T hydroquinone from the synthesis.^[27] $\Delta H_{m,U}$ (the change in energy from the melting of unstretched samples) values in Table 2 indicate the relative levels of crystallinity present in each sample. The 1/5 series was seen to crystallize more than the 1/3 pair, which was probably because of the greater aliphatic component. The addition of T in both cases was seen to depress crystallinity. In the 1/5 series, modifications to the T unit further depressed crystallinity.

The results of the tensile mechanical testing of melt-pressed films are summarized in Table 3. All three iptycene-containing polyesters displayed about twice the Young's modulus, more than twice the strength, and 14–20 times the strain to failure compared with the reference polyester (Fig. 4).

Table 2. Thermal properties of polyesters.

| Sample | ρ [g/cc] [a] | T_g [°C] [b] | T_m [°C] [c] | $\Delta H_{m,U}$ [J g ⁻¹] [c] | $\Delta H_{m,S}$ [J g ⁻¹] [c] | T_d [°C] [d] |
|-----------|-------------------|----------------|----------------|---|---|----------------|
| 1/3 R [e] | 1.20 | 25 | 119 | 28 | N/A | 375 |
| 1/3 T [e] | 1.18 | 55 | 93 | 12 | N/A | 382 |
| 1/5 R | 1.19 | 26 | 123 | 35 | N/A | 372 |
| 1/5 T | 1.18 | 52 | 102 | 27 | 34 | 380 |
| 1/5 NpT | 1.17 | 55 | 100 | 24 | 29 | 384 |
| 1/5 TbT | 1.14 | 57 | 97 | 9 | 12 | 376 |

[a] Taken by researchers at DuPont (± 0.01). [b] 1 Hz $\tan(\delta)$ ($\tan(\delta)$ = loss modulus/storage modulus) curve of Dynamic Mechanical Analysis (DMA). [c] DSC—U: unstretched isotropic films; S: films that were strained to failure; and N/A: data not taken. [d] Thermogravimetric analysis (TGA) of powders in air and assumed to be independent of processing conditions. [e] Data from the previous study on solvent-cast films.^[26]

Table 3. Tensile properties of polyester films.

| Sample | E [GPa] | σ [MPa] | ϵ_b [%] | Work [J cm ⁻³] | m_{WH} [a] |
|-----------|-----------------|----------------|------------------|----------------------------|--------------|
| 1/3 R [c] | 0.58 \pm 0.03 | 17 \pm 1 | 10 \pm 2 | 1.5 \pm 0.3 | – |
| 1/3 T [c] | 1.62 \pm 0.11 | 42 \pm 4 | 211 \pm 17 | 66.3 \pm 8.3 | 0.15 [b] |
| 1/5 R | 0.63 \pm 0.09 | 22 \pm 1 | 16 \pm 8 | 2.7 \pm 0.6 | – |
| 1/5 T | 1.39 \pm 0.27 | 54 \pm 10 | 336 \pm 45 | 101.0 \pm 11.3 | 0.20 [b] |
| 1/5 NpT | 1.38 \pm 0.63 | 54 \pm 10 | 284 \pm 32 | 83.8 \pm 0.6 | 0.26 [b] |
| 1/5 TbT | 1.15 \pm 0.56 | 46 \pm 5 | 219 \pm 24 | 56.2 \pm 4.2 | 0.24 [b] |

[a] m_{WH} = slope of stress–strain curve in the work-hardening (WH) regime. [b] Standard deviations for these values were all around ± 0.005 . [c] Data from the previous study on solvent-cast films.^[26]

Table 4. WAXS D spacings of 1/5 polyester films.

| Sample | Peaks [Å] | | | | | | | | |
|---------|-----------|-----|-----|---------|-----|-----|-----|-----|-----|
| | 1 | 2 | 3 | 4' | 4 | 5' | 5 | 6 | 7 |
| R [a] | 15.7 | 5.5 | 5.0 | 4.5 | 4.2 | 3.8 | 3.7 | 3.4 | 3.0 |
| T [a] | 15.6 | 5.5 | 5.0 | – | 4.2 | 3.9 | – | – | – |
| NpT [a] | 15.6 | – | – | – | 4.2 | – | – | – | – |
| TbT [a] | – | – | – | 4.6 [b] | – | – | – | – | – |

[a] Measured from circular integrations. [b] Could be a superposition of peaks 3 and 4.

The addition of iptycene units to the backbone of the polyester did not change the type of crystal formed because all detectable reflections in wide-angle X-ray scattering (WAXS) matched those already present in the reference polyester (Table 4). This indicates that the non-iptycene segments are responsible for the crystallization.

WAXS images are shown in Figure 5, and equatorial scans of the strained films were superimposed onto circular integrations of the unstrained films in Figure 6. The reference NT polyester did not strain significantly before failure, so an X-ray of that strained sample was not taken. The decrease in sharpness and relative number of rings evident in Figure 5 also confirms the trend of decreasing crystallinity with size of iptycene unit that was shown by using DSC. The peak (equatorial arc) positions

of the strained samples were 4.1, 4.1, and 4.3 Å for the T polyester, the NpT polyester, and the TbT polyester, respectively. The full width half maximum (FWHM) of this peak from equatorial scans (Fig. 6) of the samples were 3.9, 4.1, and 4.6 nm⁻¹ for T, NpT, and TbT, respectively. This confirms that the films that strained less before failure exhibited less molecular orientation in the loading direction, as expected.

The T polyester presents the best enhancement of stiffness, strength, and ductility. The increased stiffness of the iptycene-containing polyesters occurred despite the decrease in crystallinity (compared to the reference polyester), because the iptycene units stiffened the chain backbone, which was evident from the rise in T_g . It might be tempting to attribute the higher stiffness and ductilities of the iptycene-containing polyesters solely to the increase in T_g and decrease in crystallinity. But this correlation was not supported when comparing the iptycene-containing polyesters to one another. The 1/3 T polyester had a higher T_g and lower crystallinity than the 1/5 T polyester. But, although the

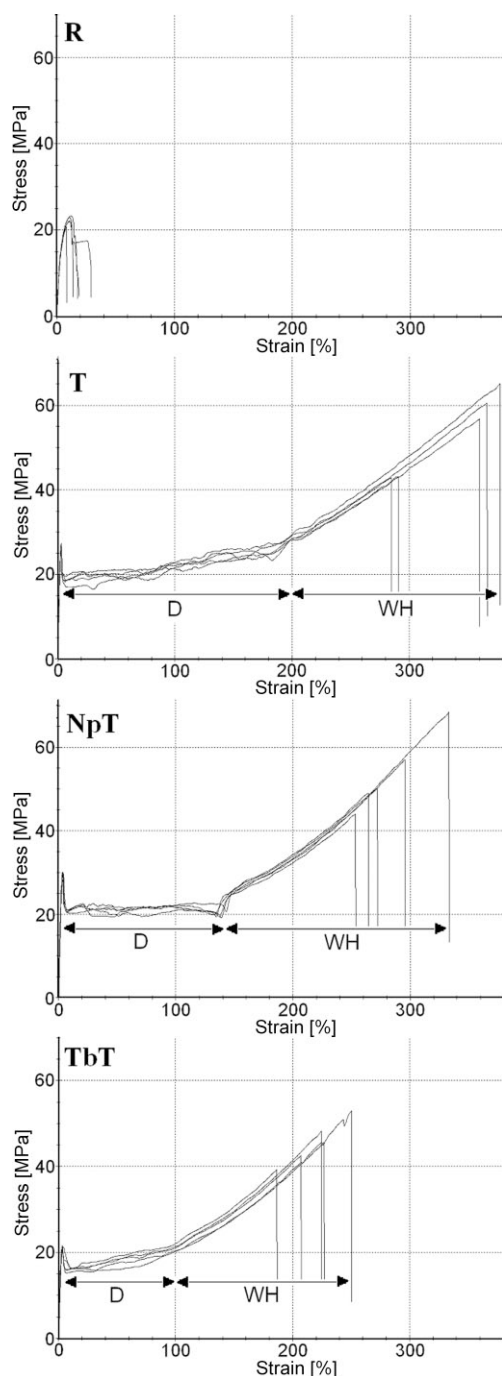


Figure 4. Tensile stress–strain curves of 1/5 polyester films. Two deformation regimes are specified in the ductile films (D=drawing; WH=work hardening).

modulus of the 1/3 T polyester was increased, the ductility suffered significantly. Additionally, amongst the 1/5 iptycene-containing polyesters (T, NpT, TbT), the increase in T_g and decrease in crystallinity lead to decreased modulus and decreased strain to failure. The two reference polyesters also negated such a suggested correlation as the 1/5 R (R=reference) exhibited better stiffness, strength, and ductility com-

pared to the 1/3 R, although it had higher crystallinity and about the same T_g , molecular weight, and chain contour.

To explain the variations in the mechanical behavior of these polymers, we focus on the effects of the presence of pendant iptycene units with their IMFV and the tendency for molecular threading and interlocking. The bulky iptycene units stiffen the backbone of the polymer chain itself, but the minimization of IMFV also results in the occupation of iptycene clefts by neighboring polymer chains. This combination together significantly restricts chain dynamics, which accounts for the large increase in T_g compared with the reference polyester. The differences in T_g between the various iptycene-containing polyesters was relatively insignificant compared to what might be expected given the large differences in the inherent IMFV calculated for the various isolated iptycene units (Fig. 1). The variation of the mechanical stiffness of the 1/5 iptycene films seemed to correlate with their differences in crystallinity. However, this was not the case with ductility.

The NpT polyester failed at notably smaller strains than the T polyester, and the TbT polyester failed at even lower strains. As expected, all three polymers exhibited levels of molecular orientation commensurate with their respective strain-to-failure values. Typically, less-oriented samples yield lower stress levels because the stress–strain behavior in the work-hardening (WH) regime is caused by the entropic penalty associated with the uncoiling and alignment of polymer chains.^[28–33] This assumes no effects from crystallinity. A polymer developing less chain orientation with applied strain generally has a lower WH slope (m_{WH}). However, our experimental values show the opposite trend. Both the NpT and TbT polyesters exhibited increased WH slopes (Table 3), despite lower final orientation states. These results cannot be attributed to crystallinity because both the NpT and TbT polyesters have less crystallinity than the T polyester (with no signs of strained-induced crystallinity). Therefore, we attribute the increase in slope to the more extensive molecular interlocking of iptycene units, which represents an additional (and new) work-hardening mechanism specific to these types of molecular barbed-wire polymers.

To investigate the interlocking mechanism further, the post-yield deformation was divided into two distinct behavioral regimes: drawing (D) and WH. These regimes are labeled on the stress–strain curves in Figure 4, using the abrupt change in slope of the stress–strain profile to identify each region. These two regimes correspond to particular types of behavior directly related to the ideas of threading and interlocking induced by the molecular-barbed-wire contour of the polymer chains.^[26] The D regime relates to the threading mechanism. The onset of iptycene interlocking likely occurs during the latter stages of D. The WH region begins when the combination of entropic forces and this new interlocking mechanism dominates the mechanical response of the material. It can be seen from the present study that, as the size of the pendant iptycene unit increased, the total D strain decreased and was accompanied by the earlier initiation of the WH regime. The NpT polyester displayed significantly less total D than the T polyester but

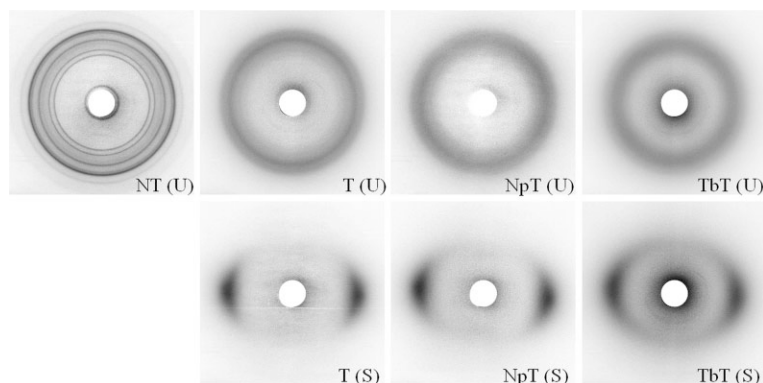


Figure 5. 2D WAXS patterns of unstretched (U) and strained to failure (S) 1/5 melt-processed films. R(S) was not taken because of the low failure strains.

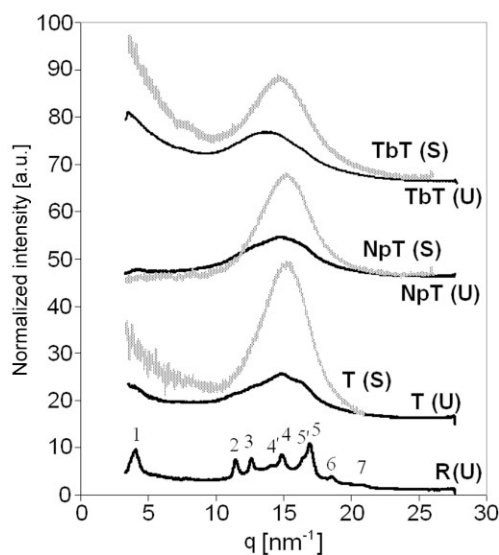


Figure 6. WAXS circular integrations of unstretched (U) 1/5 films and equatorial integrations with a width of 10 azimuthal degrees after strain to failure (S). X-ray patterns of R(S) were not taken because of the low failure strains in the NT polymer.

maintained the same level of total WH strain representing a greater contribution of the WH regime to the total post-yield deformation. The shortening of the D regime could be anticipated, as the NpT is a physically larger unit. The molecular interlocking of such units would contribute to the mechanical behavior at lower strains than the T unit because of the greater resistance to deformation. This is also likely to be why the NpT polyester has the larger m_{WH} despite exhibiting less chain orientation. In this case, the additional resistance to deformation from molecular interlocking dominated over the reduced entropic force (from less chain orientation) resulting in the higher measured stress levels at any given strain in the WH regime.

The TbT polyester transitioned into its WH regime at even smaller strains but then expressed a much-shortened total WH strain. The slope of this regime for the TbT polyester was

slightly lower than that for the NpT polyester but was still notably higher than for the T polyester. This again can be attributed to the interplay between the entropic penalty of uncoiling/aligning polymer chains and the molecular interlocking of iptycene units. The interlocking of the larger units results in the earlier initiation of the WH regime and a lower degree of final chain orientation. It can be seen from Figure 5 that the *unstrained* TbT had a WAXS halo centered on a higher d -spacing (a lower q vector—the scattering vector in reciprocal space: peak 4 for T, NpT versus peak 4' for TbT in Table 4) than the other T samples, which could be an indication that the TbT unit was not as effective at promoting molecular threading as either the T or NpT units in the prepared isotropic samples. Therefore, we suggest that the decrease in the D regime was not only because of the

earlier significance of interlocking but also because of decreased amounts of threading. The m_{WH} of the TbT polyester was higher than that of the T polyester because the increased stress contribution from the molecular interlocking of bigger iptycene units dominated over the reduced entropic force from less chain orientation. However, the m_{WH} of the TbT polyester was slightly lower than that of the NpT polyester. In comparing these two, the reduced entropic force must have outweighed the gain in stress produced by the molecular interlocking of the larger iptycene unit.

Why were the T and NpT polymers more suited for molecular threading than the TbT polymer? Although structural units with higher amounts of inherent IMFV (calculated in Fig. 1) might be expected to induce greater amounts of molecular threading, it is critical to note the accessibility of the cavities that are assumed to be occupied by neighboring chains. In the case of the NpT, the IMFV of a pendant unit probably has the same accessibility as a T unit. However, a larger cavity may not promote any more threading than is already present in the T. The TbT has even larger amounts of inherent IMFV, but, in this case, accessibility might be a significant problem because of the rotational freedom of the *tert*-butyl groups. The molecular dynamics of these groups could sterically obstruct the occupation of empty cleft spaces by shielding the opening. It is possible that during deformation, *tert*-butyls could momentarily cease to obstruct a cleft space. Once a chain slides into that cavity, it can then begin threading along the iptycene, and it is unlikely to vacate that space. The peak shift to a higher q -vector for the TbT polyester during deformation was greater than for both of the other samples ($\Delta q_{TbT} \approx 3\Delta q_T$, $\Delta q_T \approx \Delta q_{NpT}$), which could be an indication that threading was indeed increasing during deformation. However, given the early initiation of the WH regime, it is likely that some of the iptycene clefts remained unoccupied even at failure. Therefore, even though the TbT polyester here had the most *inherent* IMFV, that calculation only considers a static, isolated structural unit. An *effective* IMFV would take into account chain dynamics and the particular incorporation into a polymer backbone. In this case, the effective IMFV may have been much lower than the inherent IMFV calculation.

The contribution of molecular interlocking to a sample's ability to resist applied load will also depend on the concentration of pendant units. The m_{WH} of the 1/3 T polyester was much lower than any of the 1/5 iptycene polyesters studied, despite having more units presumably capable of interlocking (1/3 T \approx 21 wt % T versus 1/5 T \approx 15 wt % T). This was again because of the lower strain to failure, which reduced the entropic contribution to the stress in the WH regime. The pendant concentration also affects other structural and mechanical characteristics, as might be expected. Integration of the crystalline peak in DSC ($\Delta H_{\text{m,U}}$) showed that the greater concentration of T resulted in a larger depression of crystallinity relative to each polymer's reference NT counterpart. Specifically, the addition of 15 wt % T produced a 23 % decrease in relative crystallinity, whereas the addition of 21 wt % T produced a 57 % drop in relative crystallinity. The greater concentration of T also slightly increased T_g , but only by 3 °C. Most interestingly, despite the greater reduced crystallinity, the 21 wt % T content produced an almost three times higher modulus than the reference polyester, whereas the 15 wt % T content produced closer to two times higher modulus than its reference polyester. It is interesting to note that the relative contributions of each deformation regime to the total sample strain (D:WH ratio) were approximately the same for the 1/3 and 1/5 T polyesters. In a system where the contributions of chain orientation to the deformation resistance in the WH regime are known, it would be possible to isolate the additional forces associated with molecular interlocking. Once empirical values for the contribution of molecular interlocking are attained, an interlocking index can be created to correlate the size, shape, and frequency of pendant units to the stress-strain behavior in the WH regime.

3. Conclusions

In summary, the incorporation of rigid pendant units with IMFV (in contrast to conventional smooth polymer-chain-contour systems) significantly improved the mechanical properties of a family of polyesters. Our results further established the idea that threading and interlocking of polymer chains through molecular-level steric interactions is a novel means to enhance ductility and simultaneously increase stiffness and strength. The accessibility of the incorporated IMFV plays an important role in exploiting these new mechanisms. Mechanical data suggest that the amount of IMFV, as well as the size and shape of the pendant unit, must be optimized within the polymer system and that larger IMFV units are *not* necessarily better. Additionally, it was demonstrated that molecular interlocking can create a stronger system than can be produced considering only chain orientations and crystallinity. The stress response at any particular strain was enhanced by simply modifying the T unit. Therefore, these types of systems can be used to meet different application requirements for particular strength values by specific strains by making only minor changes to the iptycene unit. Finally, the degree of molecular threading and the onset of molecular interlocking determine the ratio of the D to WH

regimes (D:WH), which were found to be dependent on the size and shape of the particular iptycene unit. In the future, it may be possible to use these ratios to index propensities for certain pendant groups with IMFV to induce molecular threading and interlocking.

4. Experimental

Material Synthesis: The intermediate hydroquinones were synthesized by using a Diels–Alder reaction between tetracene, 2,6-bis-*t*-butylanthracene, or anthracene and benzoquinone using a reported procedure [26], with a yield of ca. 90 % after two steps. The hydroquinone was then reacted with trimethylsilyl chloride in the presence of imidazole in tetrahydrofuran (THF) to obtain bis(trimethylsilyl)-protected monomers. These intermediates have sufficiently low melting points and, upon the addition of a catalytic amount of pyridine hydrochloride, were easily deprotected in situ in the molten state. NpT polyester was obtained from the reaction of bis(trimethylsilyl)-protected mononaphthotriptycene, the chain extender (1,10-bis(trimethylsilyloxy)decane), and terephthaloyl chloride. Likewise, TbT polyester and T polyester were prepared from the corresponding bis(trimethylsilyl)-protected T. The NT polyester (NT) was prepared from a reaction of bis(trimethylsilyl)hydroquinone, the chain extender (1,10-bis(trimethylsilyloxy)decane), and terephthaloyl chloride.

Mononaphthotriptycene-1,4-hydroquinone: Adapting a published procedure [26], tetracene (2.0 g, 8.76 mmol) and benzoquinone (1.23 g, 11.4 mmol) was added to a flask containing 30 mL of xylene. The mixture was refluxed under nitrogen for 1 h and cooled to room temperature. The solvent was removed and the solid was washed with hot water to remove quinone and hydroquinone. ^1H NMR of the resulting solid had a complex pattern in the aromatic region. IR spectroscopy (KBr) confirmed the presence of a carbonyl group ($\text{C}=\text{O}$, $\nu=1692\text{ cm}^{-1}$), indicating that simple Diels–Alder products that had not isomerized to the hydroquinone were present. The crude mixture was added to a flask containing glacial acetic acid (20 mL) and the mixture was brought to 100 °C. Five drops of 40 % hydrobromic acid were added and the solution was refluxed for 1 h. The mixture was cooled and filtered. The product was recrystallized from acetone/dichloromethane to obtain 2.65 g (90 % overall) of white solid. ^1H NMR (acetone- d_6 , δ): 6.10 (s, 2H), 8.0 (s, 2H), 7.86 (s, 2H), 7.72–7.74 (m, 2H), 7.51–7.36 (m, 2H), 7.39–7.36 (m, 2H), 7.04–7.01 (m, 2H), 6.47 (s, 2H), 6.10 (s, 2). ^{13}C NMR (Acetone- d_6 , δ): 145.6, 145.5, 143.2, 132.3, 132, 127.6, 125.7, 125.4, 121.7, 116, 113.4. IR, (KBr, Ar–OH, cm^{-1}): 3286. The crude material was crystallized from acetone/dichloromethane to obtain hydroquinone with 75 % yield.

Mononaphtho-1,4-di(trimethylsilyloxy) Triptycene: Mononaphthotriptycene-1,4-hydroquinone (1.10 g, 3.27 mmol) and imidazole (0.52 g, 7.85 mmol) were placed in a 100 mL flask with a magnetic stir bar under nitrogen. Dry THF (50 mL) was added via a cannula and the solution was stirred at room temperature to obtain a clear solution. Chlorotrimethylsilane (1.0 mL, 9.4 mmol) was added and the reaction was heated to reflux with stirring for 10 h. The resulting mixture was cooled to room temperature and filtered. The white solid was washed with hexane and the washing was combined with the filtrate. The solvents were removed in vacuo and the remaining solid was passed through a short bed of silica gel using 15 % dichloromethane in hexane. This solvent was removed under reduced pressure to obtain a white solid product (1.50 g, 96 %). ^1H NMR (CDCl_3 , δ): 7.78 (s, 2H), 7.73–7.71 (m, 2H), 7.45–7.36 (m, 4H), 7.04–7.01 (m, 2H), 6.4 (s, 2H), 5.83 (s, 2H), 0.34 (s, 18H). ^{13}C NMR (CDCl_3 , δ): 154.2, 144.7, 142.6, 136.1, 131.9, 127.7, 125.7, 125.5, 124.2, 122.0, 117.5, 47.9, 0.89. Elemental analysis calculated for $\text{C}_{30}\text{H}_{32}\text{O}_2\text{Si}_2$: C: 74.95, H: 6.71; found C: 74.94, H: 6.69.

2,6-di-*tert*-Butyl-1,4-di(trimethylsilyloxy)triptycene: This compound was produced in 94 % yield from the corresponding triptycene hydroquinone [34] (1.5 g, 3.76 mmol), imidazole (0.63 g, 9.4 mmol), and chlorotrimethylsilane (1.18 mL, 9.4 mmol (1.94 g)). ^1H NMR (CDCl_3 , δ): 7.45 (s, 2H), 7.31–7.29 (d, 2H), 7.02–6.99 (m, 2H), 6.37 (s, 2H), 5.67

(s, 2H), 1.23 (s, 18H), 0.33 (s, 18H). ^{13}C NMR (CDCl_3 , δ): 147.8, 145.8, 144.7, 144.4, 143.1, 137.54, 137.47, 123.3, 121.6, 121.5, 117.4, 117.1, 49.1, 47.4, 34.8, 31.8, 0.93. Elemental analysis calculated for $\text{C}_{34}\text{H}_{46}\text{O}_2\text{Si}_2$: C: 75.22, H: 8.54; found C: 75.20, H: 8.51.

Polymer Synthesis: The T polyester was synthesized by melt-polymerization. Appropriate ratios of 1,4-di(trimethylsilyloxy)-mononaphthotriptycene, 1,10-bis(trimethylsilyloxy)decane, and terephthaloyl chloride were mixed under nitrogen in a Schlenk flask. The flask was closed with a septum and heated to 170 °C with stirring until the mixture gave a yellowish liquid. The addition of a catalytic amount of pyridine hydrochloride to the molten mixture resulted in situ deprotection of compounds that were then reacted with terephthaloyl chloride. Pyridine hydrochloride was added in three portions in about 20 min time intervals. The flask was frequently vented through a needle while the reaction was under a positive pressure of nitrogen. A viscous mixture was formed after about one hour and the reaction was continued under vacuum for 12 h, after which the mixture was cooled to room temperature. The solid formed was dissolved in THF and filtered through a medium sintered glass funnel to remove insoluble materials. The clear filtrate was precipitated into methanol. The white solid precipitate collected was washed with methanol and dried in a vacuum at 50 °C overnight. Yields were typically ca. 95 %.

Naphthalene-Modified Triptycene Polyester: The same procedure was used to produce the polymer from bis(trimethylsilyl)-protected mononaphthotriptycene (0.179 g, 0.372 mmol, 1 eq), 1,10-bis(trimethylsilyloxy)decane (0.593 g, 1.862 mmol, 5 eq), and terephthaloyl chloride (0.453 g, 2.231 mmol, 6 eq). This yielded 0.70 g of product after precipitation from methanol (MeOH) (95 % yield). ^1H NMR (CDCl_3 , δ): 8.44–8.36 (t, 2H), 8.35–8.26 (t, 2H), 8.05 (s, 10H), 7.42–7.20 (m, 4 H), 7.15–6.90 (m, 2H), 4.45–4.35 (m, 13H), 1.9–1.7 (m, 13H), 1.6–1.2 (m, 52H).

tert-Butyl-Modified Triptycene Polyester: This polymer was synthesized similarly from 2,6-di-tert-butyl-1,4-bis(trimethylsilyloxy)triptycene (0.90 g, 1.657 mmol, 1 eq), 1,10-bis(trimethylsilyloxy)decane (2.641 g, 8.288 mmol, 5 eq), and terephthaloyl chloride (2.018 g, 9.94 mmol, 6 eq). We isolated 3.24 g of product after precipitation from MeOH (95 % yield).

Triptycene Polyester: This was synthesized in a similar fashion from 1,4-bis(trimethylsilyloxy)triptycene (5.016 g, 11.646 mmol, 1 eq), 1,10-bis(trimethylsilyloxy)decane (18.556 g, 58.232 mmol, 3 eq), and terephthaloyl chloride (14.186 g, 69.878 mmol, 4 eq). The product (21.9 g) was recovered after precipitation from MeOH (97 % yield). ^1H NMR (CDCl_3 , δ): 8.60 (m, 0.33H), 8.41 (m, 2H), 8.29 (m, 2H), 8.11 (m, 20H), 7.36 (m, 4H), 7.03 (m, 4H), 6.94 (m, 1.66H), 5.51 (m, 2H), 4.42 (m, 4H), 4.34 (m, 20H), 1.80 (m, 24H), 1.34 (m, 72H).

Non-Triptycene Polyester: This polymer was synthesized from 1,4-bis(trimethylsilyloxy)benzene (0.885 g, 3.477 mmol, 1 eq), 1,10-bis(trimethylsilyloxy)decane (5.54 g, 17.417 mmol, 5 eq), and terephthaloyl chloride (4.243 g, 20.897 mmol, 6 eq). The product (5.72 g) was obtained after precipitation from MeOH (93 % yield). ^1H NMR (CDCl_3 , δ): 8.38 (s, 0.16H), 8.27 (m, 4H), 8.20 (m, 4H), 8.10 (s, 20H), 7.32 (m, 3.8H), 4.35 (m, 20H), 1.78 (m, 20H), 1.42 (m, 60H).

Characterization: Samples were scanned at 10 °C min $^{-1}$ with TA Instruments Q1000 differential scanning calorimeter to obtain values for the melting temperature and enthalpy of melting according to ASTM D3418-03 (ASTM = American Society for Testing and Materials). The glass-transition temperatures were not evident from the DSC, but could be determined from the $\tan(\delta)$ ($\tan(\delta)$ = loss modulus/storage modulus) versus temperature plots using dynamic mechanical analysis. TGA was used to determine degradation temperatures in air at a heating rate of 5 °C min $^{-1}$ with Q50 thermogravimetric analyzer from TA Instruments. The values for the temperatures at which the highest amount of degradation occurred were obtained from the first derivative of the sample weight versus temperature curve. These were reported as the T_d . Density measurements were taken using a Micromeritics AccuPyc 1330 He pycnometer by researchers at DuPont.

Samples were first dissolved in dichloromethane at 60 °C at concentrations of roughly 12 mg mL $^{-1}$. Solutions were then transferred through Target 0.2 μm Teflon filters into custom-machined, rectangular Teflon dishes and allowed to evaporate slowly for 48 h at room temper-

ature with a glass cover. To ensure the elimination of all of the solvent, the films were then placed in a vacuum oven at 65 °C for 5 h. This procedure produced films of 100–120 μm thickness. To melt-press the samples, solvent-cast films were pressed at roughly 1000 psi at 150 °C for about 5 min in a Carver hydraulic hot press and then cooled by coils running cold water through the platens. This produced films of approximately 70–100 μm thickness. These films were cut with a razor blade into test samples of about 3–4 mm width and 50 mm in length. Cut films were stored under vacuum for a month to ensure the same level of dryness from sample to sample. A TA Instruments Q800 Dynamic Mechanical Analyzer was used to acquire $\tan(\delta)$ for the films in tension. Films were cyclically strained at about 0.1–0.2 % engineering strain at frequencies of 1 Hz and 10 Hz using a temperature ramp rate of 2 °C min $^{-1}$. 2–3 films were tested per sample. A Zwick/Roell Z010 with a 500 N load cell and PN8133 grips was used to determine the tensile mechanical properties of the prepared films. Using a gauge length of 40 mm and a preload of 0.02 N, films were strained to failure at a rate of 40 mm min $^{-1}$. The Zwick software was used to determine the Young's modulus, strength, and strain to failure of the films. Mechanical properties data are presented as an average of five tested samples. The regions of D and WH were determined by a change in slope in the post-yield engineering stress–strain curves. The slope of the WH regime was calculated using only the final 50 % strain.

WAXS patterns were taken at the X27C beamline at the Brookhaven National Synchrotron Light Source. All images were normalized for sample thickness, exposure time, and beam flux, and then cropped for the figures. D spacings were calibrated with silver behenate using Polar Software. Accelrys Materials Studio modeling software was used to construct the T, NpT, and TbT models and to calculate the volume occupied by the units using a van der Waals isosurface.

Received: July 31, 2006

Revised: November 10, 2006

Published online: April 30, 2007

- [1] M. G. Northolt, J. J. M. Baltussen, B. Schafferskorff, *Polymer* **1995**, 36, 3485.
- [2] M. G. Northolt, J. J. M. Baltussen, *J. Appl. Polym. Sci.* **2002**, 83, 508.
- [3] D. J. Sikkema, *J. Appl. Polym. Sci.* **2002**, 83, 484.
- [4] T. Kikutani, *J. Appl. Polym. Sci.* **2002**, 83, 559.
- [5] H. Uehara, Y. Yamazaki, T. Kanamoto, *Polymer* **1996**, 37, 57.
- [6] P. J. Flory, *Principles of Polymer Chemistry*, Cornell University Press, Ithaca **1953**.
- [7] R. J. Young, P. Lovell, *Introduction to Polymers*, 2nd ed., Chapman and Hall, London **1991**.
- [8] S. Fakirov, M. Evstatiev, J. M. Schultz, *J. Appl. Polym. Sci.* **1991**, 42, 575.
- [9] D. W. Grijpma, H. Altpeter, M. J. Bevis, J. Feijen, *Polym. Int.* **2002**, 51, 845.
- [10] J.-H. Jang, C. K. Ullal, T. Choi, M. C. Lemieux, V. V. Tsukruk, E. L. Thomas, *Adv. Mater.* **2006**, 18, 2123.
- [11] D. J. Sikkema, M. G. Northolt, B. Pourdeyhimi, *MRS Bull.* **2003**, 28, 579.
- [12] Y. H. So, *Prog. Polym. Sci.* **2000**, 25, 137.
- [13] S. H. Wu, *Polym. Int.* **1992**, 29, 229.
- [14] D. J. Liaw, B. Y. Liaw, J. R. Chen, C. M. Yang, *Macromolecules* **1999**, 32, 6860.
- [15] D. J. Liaw, B. Y. Liaw, C. M. Yang, *Macromolecules* **1999**, 32, 7248.
- [16] Y. Oishi, M. Ishida, M. A. Kakimoto, Y. Imai, T. Kurosaki, *J. Polym. Sci. Part A: Polym. Chem.* **1992**, 30, 1027.
- [17] K. H. Park, T. Tani, M. A. Kakimoto, Y. Imai, *J. Polym. Sci. Part A: Polym. Chem.* **1998**, 36, 1767.
- [18] M. Dotrong, M. H. Dotrong, H. H. Song, U. Santhosh, C. Y. C. Lee, R. C. Evers, *Polymer* **1998**, 39, 5799.
- [19] T. R. Kelly, J. P. Sestelo, I. Tellitu, *J. Org. Chem.* **1998**, 63, 3655.
- [20] H. Iwamura, K. Mislow, *Acc. Chem. Res.* **1988**, 21, 175.

- [21] Z. G. Zhu, T. M. Swager, *J. Am. Chem. Soc.* **2002**, *124*, 9670.
- [22] T. M. Long, T. M. Swager, *Adv. Mater.* **2001**, *13*, 601.
- [23] T. M. Long, T. M. Swager, *J. Am. Chem. Soc.* **2002**, *124*, 3826.
- [24] J. S. Yang, T. M. Swager, *J. Am. Chem. Soc.* **1998**, *120*, 5321.
- [25] D. Zhao, T. M. Swager, *Macromolecules* **2005**, *38*, 9377.
- [26] N. T. Tsui, L. Torun, A. J. Paraskos, T. M. Swager, E. L. Thomas, *Macromolecules* **2006**, *39*, 3350.
- [27] K. Yamamura, T. Kawashima, K. Eda, F. Tajima, M. Hashimoto, *J. Mol. Struct.* **2005**, *737*, 1.
- [28] R. N. Haward, G. Thackray, *Proc. R. Soc. London Ser. A* **1968**, *302*, 453.
- [29] J. G. Rider, E. Hargreaves, *J. Polym. Sci.* **1969**, *7*, 829.
- [30] A. S. Argon, *Philos. Mag.* **1973**, *28*, 839.
- [31] D. J. Brown, A. H. Windle, *J. Mater. Sci.* **1984**, *19*, 1997.
- [32] I. M. Ward, *Polym. Eng. Sci.* **1984**, *24*, 724.
- [33] M. C. Boyce, E. M. Arruda, *Polym. Eng. Sci.* **1990**, *30*, 1288.
- [34] T. M. Long, T. M. Swager, *J. Am. Chem. Soc.* **2003**, *125*, 14113.
-